Mutations in the nervous system–specific *HSN2* exon of *WNK1* cause hereditary sensory neuropathy type II

Masoud Shekarabi,[1] Nathalie Girard,[1] Jean-Baptiste Rivière,[1] Patrick Dion,[1] Martin Houle,[2] André Toulouse,[1] Ronald G. Lafrenière,[1] Freya Vercauteren,[1] Pascale Hince,[1] Janet Laganiere,[1] Daniel Rochefort,[1] Laurence Faivre,[3] Mark Samuels,[1] and Guy A. Rouleau[1]

[1]Centre of Excellence in Neuromics, University of Montreal, Centre Hospitalier de l'Université de Montréal, Montreal, Quebec, Canada. [2]McGill Cancer Centre, Montreal, Quebec, Canada. [3]Centre de Génétique, Hôpital d'Enfants, Dijon, France.

Hereditary sensory and autonomic neuropathy type II (HSANII) is an early-onset autosomal recessive disorder characterized by loss of perception to pain, touch, and heat due to a loss of peripheral sensory nerves. Mutations in hereditary sensory neuropathy type II (*HSN2*), a single-exon ORF originally identified in affected families in Quebec and Newfoundland, Canada, were found to cause HSANII. We report here that *HSN2* is a nervous system–specific exon of the with-no-lysine(K)–1 (*WNK1*) gene. *WNK1* mutations have previously been reported to cause pseudohypoaldosteronism type II but have not been studied in the nervous system. Given the high degree of conservation of *WNK1* between mice and humans, we characterized the structure and expression patterns of this isoform in mice. Immunodetections indicated that this *Wnk1/Hsn2* isoform was expressed in sensory components of the peripheral nervous system and CNS associated with relaying sensory and nociceptive signals, including satellite cells, Schwann cells, and sensory neurons. We also demonstrate that the novel protein product of *Wnk1/Hsn2* was more abundant in sensory neurons than motor neurons. The characteristics of *WNK1/HSN2* point to a possible role for this gene in the peripheral sensory perception deficits characterizing HSANII.

Introduction

Hereditary sensory neuropathies form part of the inherited peripheral neuropathies that are subdivided into 3 categories, depending on the selective or predominant involvement of the motor or sensory peripheral nervous system (PNS) (1). The most common of these neuropathies affect both motor and sensory nerves. In the second category, only the peripheral motor nervous system is affected, and the neuropathy is classified as a distal hereditary motor neuropathy. Finally, there are neuropathies in which sensory dysfunction prevails, and these are referred to as hereditary sensory and autonomic neuropathies (HSANs). Hereditary sensory and autonomic neuropathy type II (HSANII; OMIM 201300) is an early-onset autosomal recessive disorder. It is characterized by loss of perception to pain, touch, and heat attributable to a partial loss of peripheral sensory nerves (2–4). In 2004, we reported mutations in the hereditary sensory neuropathy type II (*HSN2*) gene, a single-exon ORF identified in Quebec and Newfoundland families, as the cause of HSANII (5). Subsequently, 3 independent groups also reported causative *HSN2* mutations in unrelated populations (6–10).

In 2001, large intronic deletions in the with-no-lysine(K)–1 (*WNK1*) gene were reported to cause Gordon hyperkalemia-hypertension syndrome, also referred to as pseudohypoaldosteronism type II (PHAII; OMIM 145260) (11). PHAII is a dominant disorder, the main feature of which is hypertension (12, 13). Members of the WNK family contain a Ser/Thr catalytic domain similar to that of other kinases. However, one of their unique characteristics is that the well-conserved lysine residue of the active domain is instead a cysteine (14). In the case of WNK1, this kinase domain extends from the end of exon 1 to exon 4. WNK1 has an autoinhibitory domain of its kinase activity (15). WNK1 has been shown to interact with a number of cellular proteins (e.g., synaptotagmin-2, MEKK2/3, protein kinase B) (16–18). Early experiments using WNK1-specific antibodies demonstrated that WNK1 is not present in all cells; rather, it was mostly localized to the polarized epithelia of the liver and kidney (19). With the exception of a recent report in which neural precursor cells were used (20) and of one in which WNK1 expression was observed in the developing brain (21), very little has been reported about WNK1 in the nervous system. Given the symptoms of PHAII patients, WNK1 experiments conducted to this day were done with kidney or liver tissues or in cellular models derived from these. We now report that *HSN2*, which was initially believed to lie within intron 8 of *WNK1*, is a nervous system–specific exon of *WNK1* that we will refer here as the *WNK1/HSN2* isoform.

Results

Compound heterozygous mutation in WNK1 and HSN2 cause HSANII. A French family (Figure 1A) was referred to G.A. Rouleau's group in Montreal by L. Faivre for an *HSN2* genetic analysis to confirm the diagnosis of HSANII in an 18-year-old female. Clinically, she had classic HSANII symptoms (2–4). Examination of the patient revealed no dysautonomia or abnormal blood pressure. Vegetative tests elicited by cutaneous stimulation revealed normal sympathetic reflexes. Parasympathetic cardiac function was found to be normal during a forced breathing test. The only apparent autonomic dysfunction observed in the patient was excessive hand sweating.

Nonstandard abbreviations used: DRG, dorsal root ganglia; HSANII, hereditary sensory and autonomic neuropathy type II; HSN2, hereditary sensory neuropathy type II; PHAII, pseudohypoaldosteronism type II; PNS, peripheral nervous system; UTR, untranslated region; WNK1, with-no-lysine(K)–1.

Conflict of interest: The authors have declared that no conflict of interest exists.

Citation for this article: *J. Clin. Invest.* **118**:2496–2505 (2008). doi:10.1172/JCI34088.

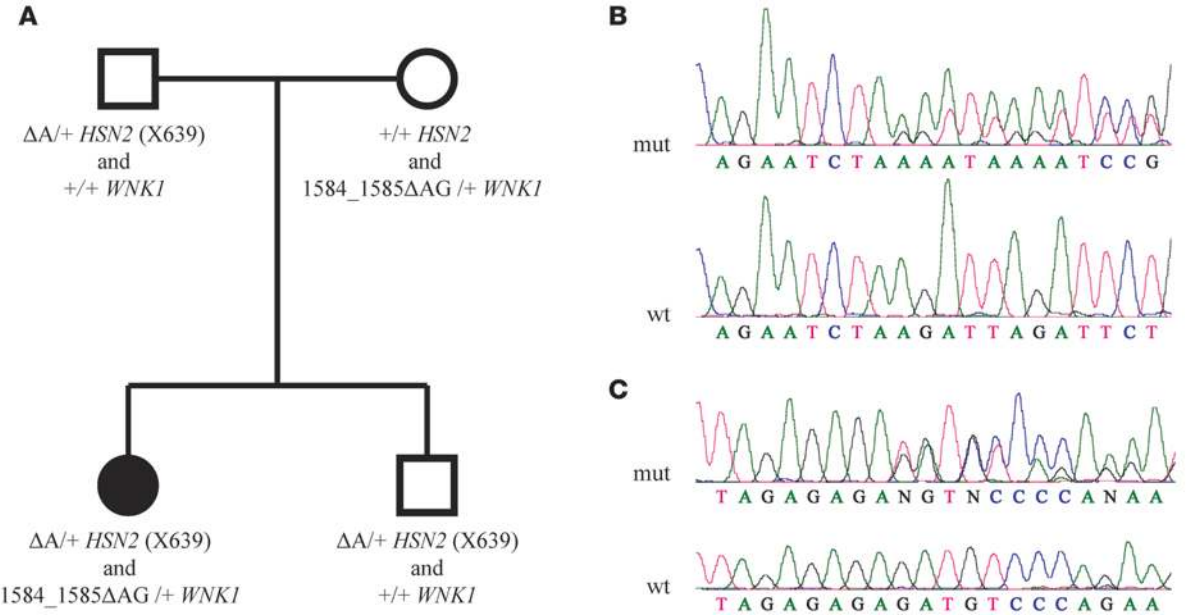

Figure 1
Mutations in the *WNK1*/*HSN2* gene. (**A**) Segregation of the 2 mutations identified in the nuclear family. The single affected individual has compound heterozygous mutations. Sequencing traces show the 1-bp deletion (639delA, Arg214fsX215) identified in *HSN2* (**B**) and the 2-bp deletion (1584_1585delAG, Asp531fsX547) identified in exon 6 of *WNK1* (**C**), with sequencing traces from a normal control. mut, mutated sequencing trace; wt, control sequencing trace.

DNA was obtained from the daughter, brother, and both parents (Figure 1A). Sequencing the *HSN2* ORF identified a heterozygous 1-bp deletion (639delA, Arg214fsX215) in the affected daughter, her asymptomatic brother, and the father (Figure 1B). Surprisingly, no other mutation could be found in *HSN2*. Despite the multiple studies (5–10) that authenticated the *HSN2* ORF as causative of HSANII and its apparent independence from *WNK1*, we decided to screen the entire coding sequence of *WNK1* and identified a second mutation (1584_1585delAG, Asp531fsX547) in exon 6 of *WNK1* (Figure 1C). This 2-bp deletion was inherited from the mother, absent in the unaffected brother, and predicted to result in a truncated protein at amino acid 547 of *WNK1*. The mother presented no abnormal blood pressure or symptoms that could be connected to HSANII. This should not be surprising, given that all *WNK1* mutations so far associated with hypertension were all large deletions in the gene's first intron that led to an overexpression of the gene (11). Given that both mother and daughter presented no obvious symptoms of abnormal blood pressure, it can be surmised that partial loss of WNK1 function has no blood pressure phenotype. The unexpected discovery of these compound heterozygous mutations in the affected daughter — one carried in *WNK1* and the other in HSN2 — led us to speculate that *HSN2* might be an alternative exon of *WNK1*, rather than an independent gene.

Nervous tissues express an HSN2 mRNA with a size similar to that of WNK1. Because the coding regions and regulatory elements of *WNK1* and *HSN2* are well conserved between mouse and human (86% identical), we used the mouse *Wnk1* orthologous gene to test our hypothesis. To detect the mRNA encoding the *Hsn2* sequence, a Northern blot of adult mouse tissues was probed with a 434-bp DNA fragment that recognized the putative 3′ coding region of *Hsn2*. A single band, with a size slightly greater than approximately 10 kb (Figure 2A, top), appeared in nervous system tissues exclusively. This band was predominant in the spinal cord, but it was also detected in the brain and dorsal root ganglia (DRG) of adult mice. At E13, the mouse embryo appears to express this mRNA in its body rather than its distal limb area and its nose area. The size of this mRNA was in accordance with observations made by 3 independent groups that detected an approximately 10.5-kb *WNK1* mRNA in the brain (14, 22, 23). A smaller kidney-specific isoform (~9.0 kb) in which exons 1–4 of *WNK1* are replaced by an alternative exon 4B has also been reported (22, 23). Our result suggests that *HSN2* is part of the *WNK1* mRNA, making it an unreported and novel nervous system–specific disease-causing isoform of *WNK1* (*WNK1/HSN2*). Past poly(A) Northern blot and RT-PCR investigation of *HSN2* failed to detect this species, because the probes and primers used were designed to recognize what were the 2 putative untranslated region (UTR) of *HSN2* (5), which now appear to be spliced out of the *WNK1/HSN2* mRNA. By comparison, *Wnk1* mRNAs that do not contain *Hsn2* sequences were detected using a *Wnk1*-specific probe in a broad range of neuronal and non-neuronal tissues (Supplemental Figure 4; supplemental material available online with this article; doi:10.1172/JCI34088DS1). Expression of *Wnk1* in DRG was previously recorded in the course of a gene expression microarray study (24).

RT-PCR shows that Hsn2 has flanking exons that are those of Wnk1. To further investigate whether *Hsn2* is an alternatively spliced exon of *Wnk1*, we performed RT-PCR reactions with primers flanking the region between the coding region of *Hsn2* and its neighboring *Wnk1* exons (Figure 2C, primers 1 and 3a for exon 8 to *Hsn2*; primers 4 and 5 for *Hsn2* to exon 10). When amplifications between *Wnk1* exon 8 and *Hsn2* were performed, a 160-bp band was visible in all neuronal tissues (Figure 2D, arrow 3) but absent from non-neuronal tissues. A very weak 160-bp band is visible in the kidney, but in light of subsequent immunodetections (see below), this may be due to contamination of the kidney sample with adrenal glands; moreover, the Northern

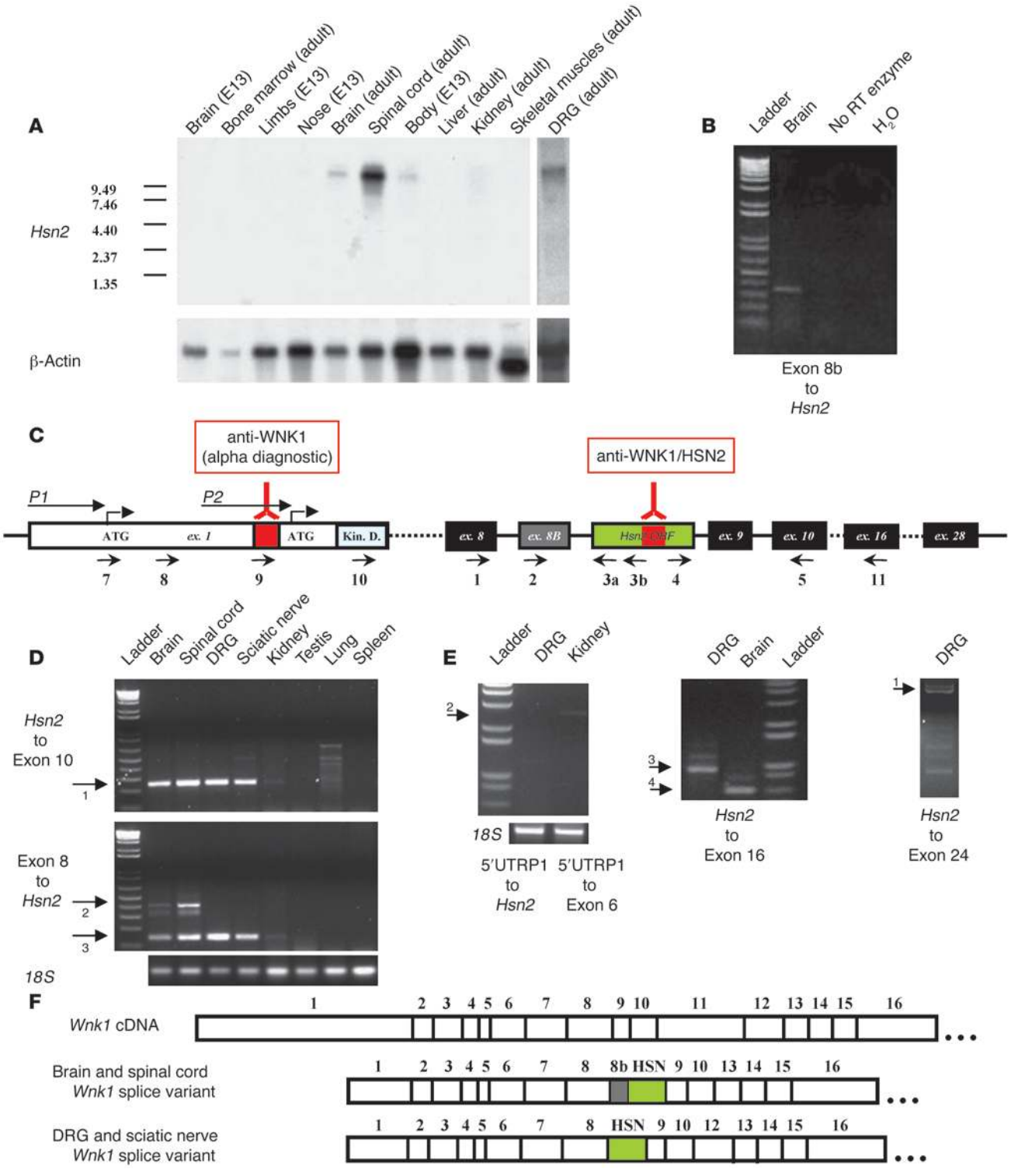
A
Brain (E13)
Bone marrow (adult)
Limbs (E13)
Nose (E13)
Brain (adult)
Spinal cord (adult)
Body (E13)
Liver (adult)
Kidney (adult)
Skeletal muscles (adult)
DRG (adult)
9.49
7.46
Hsn2
4.40
2.37
1.35
β-Actin
B
Ladder
Brain
No RT enzyme
H2O
Exon 8b
to
Hsn2
C
anti-WNK1
(alpha diagnostic)
anti-WNK1/HSN2
P1
P2
ATG
ex. 1
ATG
Kin. D.
ex. 8
ex. 8B
Hsn2 ORF
ex. 9
ex. 10
ex. 16
ex. 28
7
8
9
10
1
2
3a
3b
4
5
11
D
Ladder
Brain
Spinal cord
DRG
Sciatic nerve
Kidney
Testis
Lung
Spleen
Hsn2
to
Exon 10
1
Exon 8
to
Hsn2
2
3
18S
E
Ladder
DRG
Kidney
2
18S
5′UTRP1
to
Hsn2
5′UTRP1
to
Exon 6
DRG
Brain
Ladder
3
4
Hsn2
to
Exon 16
DRG
1
Hsn2
to
Exon 24
F
Wnk1 cDNA
1 2 3 4 5 6 7 8 9 10 11 12 13 14 15 16
Brain and spinal cord
Wnk1 splice variant
1 2 3 4 5 6 7 8 8b HSN 9 10 13 14 15 16
DRG and sciatic nerve
Wnk1 splice variant
1 2 3 4 5 6 7 8 HSN 9 10 12 13 14 15 16

Figure 2
RNA expression analyses of *Hsn2* messenger. (**A**) Northern blotting of *Hsn2* mouse tissues. The membrane was hybridized with *Hsn2* probe (top) before it was stripped and rehybridized with a β-actin probe (bottom). (**B**) RT-PCR amplifications between putative exon 8B (primer 2) and *Hsn2* (primer 3b). (**C**) Diagram of *Wnk1* encompassing *Hsn2*. Below are the numbered primers (Supplemental Table 1). The positions of *Wnk1* promoters are indicated by black arrows, and the sites detected by anti-HSN2 and anti-WNK1 (Alpha Diagnostic International) are indicated in red. Kin. D., WNK1 kinase domain. (**D**) RT-PCR amplifications from brain, spinal cord, DRG, sciatic nerve, kidney, testis, lung, and spleen cDNA. Bottom: Amplifications between exon 8 (primer 1) and *Hsn2* (primer 3a). Top: Amplifications between *Hsn2* (primer 4) and exon 10 (primer 5). Arrows 1, 2, and 3 are, respectively, at 250, 420, and 160 bp. (**E**) RT-PCR amplifications between *Hsn2* and upstream and downstream region of *Wnk1*. Left: RT-PCR between a region upstream to the 5′UTR of P1 (primer 5′UTRP1) and *Hsn2* (primer 3a) in DRG. The same panel shows the amplification between the same 5′UTR of the P1 region and exon 6 in the kidney. Middle: Amplifications between *Hsn2* (primer 4) and exon 16 (primer 11). Arrows 1, 2, 3, and 4 are, respectively, at approximately 2.2 kb, 950 bp, 650 bp, and approximately 3.8 kb. Right: Amplifications between *Hsn2* (primer 4) and exon 24 (primer not shown in **B**). (**F**) Comparison of *Wnk1*/*Hsn2* isoforms with the most common isoform of *Wnk1*.

blot analysis (Figure 2A) established the absence of *Hsn2*-containing mRNA in this organ. This 160-bp band corresponded to the predicted size of a single poly(A) species that would contain both exon 8 of *Wnk1* and *Hsn2*; this was subsequently confirmed by the sequencing. The same amplifications of the region between *Wnk1* exon 8 and *Hsn2* also yielded an additional band of approximately 420 bp in the brain and spinal cord. Sequencing of this 420-bp fragment revealed the existence of an mRNA that contained exon 8 of *Wnk1*, a novel exon downstream of exon 8 (putative exon 8B in Figure 2, C and F) and the *Hsn2* exon. The splicing of this putative exon 8B in the brain *Wnk1* mRNA was confirmed by RT-PCR reactions with primers in *Hsn2* and the putative exon 8B (Figure 2C, primers 2 and 3b), which produced a band of 320 bp (Figure 2B). The putative exon 8B encodes an ORF of 86 amino acids, and this peptide sequence was used to identify orthologous exon 8B sequences from birds, amphibians, and fish (Figure 3A). When amplifications between *Wnk1* exon 10 and *Hsn2* were prepared (Figure 2C, primers 4 and 5), a single band of 250 bp corresponding to the predicted size of a single poly(A) transcript encoding *Wnk1*'s exons 10, 9, and *Hsn2* (Figure 2D, top) was visible, again only in neuronal tissues; this was confirmed by sequencing. More RT-PCR reactions were then performed to investigate which of the more distal exons of *Wnk1* are also parts of the *Wnk1/Hsn2* isoform. In order to investigate the exons upstream to *Hsn2*, separate reactions were performed using a primer located in *Hsn2* (Figure 2C, primer 3a) and a series of primers in *Wnk1* exon 1 (Figure 2C, primers 7–10). When analyzed on agarose gel, the reactions from DRG, using primers 3a and 7, yielded a single band of approximately 2.2 kb (data not shown), and the amplifications between primers 3a and 8, 9, or 10 yielded single bands as well (data not shown). *WNK1* transcripts have been reported to be initiated from 2 distinct promoters (P1 and P2) (25); to investigate which promoter was used for the transcription of *Wnk1/Hsn2*, we used RT-PCR (Figure 2E, arrow 2). The existence of multiple *Wnk1* promoters is an important point, and multiple approaches (RT-PCRs and Western immunodetections) were necessary to establish which promoter appears to be used for WNK1/HSN2 (see Discussion). To observe the exons downstream to *Hsn2*, reactions were performed using a primer in *Hsn2* and a primer in *Wnk1* exon 16 (Figure 2C, primers 4 and 11). When loaded on gel, these amplifications revealed an approximately 650-bp band from the brain tissues and an approximately 950-bp band from the DRG (Figure 2E, arrows 3 and 4). The subsequent sequencing of these 2 fragments showed that both the brain and DRG lacked exon 11 (462 bp) and that the brain additionally lacked exon 12 (285 bp) (Figure 2F); this alternative splicing confirmed previous reports in which exons 11 and 12 were shown to be skipped in some *Wnk1* mRNAs expressed in mouse tissues (13, 23). Further amplifications of the region between the last exons of *Wnk1* and *Hsn2* were, however, more difficult because of the large distance between these primers; nonetheless, a product corresponding to the expected mRNA size (3.8 kb) could be amplified from *Hsn2* to exon 24 of *Wnk1* (Figure 2E, arrow 1). A product was also amplified from *Hsn2* to *Wnk1* exon 25, but its intensity was very weak (data not shown).

Rapid amplification of cDNA end reactions from Hsn2. To corroborate the results of the various RT-PCR products, 5′ rapid amplification of cDNA ends (5′RACE) reactions were also initiated to characterize *Wnk1/Hsn2* isoforms (with or without putative exon 8B). DNA sequencing of the region upstream to *Hsn2* confirmed the presence of a highly conserved splice junction (Figure 3B), and the mRNA did contain *Wnk1* exons 2–8 (with the inclusion of exon 8B in some cases) and the *Hsn2* exon. The distance between *Wnk1* exon 1 and *Hsn2* was too large (~2.2 kb) for the 5′RACE reaction to proceed that far from *Hsn2*. DNA sequencing of the region amplified by primers in *Wnk1* exon 10 and *Hsn2* also revealed a splice junction highly conserved across species in the region 3′ to *Hsn2* (Figure 3B). No 3′RACE reactions were done because of the size of *Wnk1*, but the gene has been reported to have 2 alternative polyadenylation sites (25). The distance between *Hsn2* and these 2 polyadenylation sites is too large (~4 kb) for direct amplifications to be possible, and this portion of *Wnk1* does not permit an easy distinction of *Wnk1/Hsn2* and *Wnk1* transcripts by PCR. It has, however, been reported that the second site appears to be more abundantly used in tissues where *WNK1* expression is high, such as the brain (25).

Western blot detection of the Wnk1/Hsn2 isoform. In order to confirm that *Hsn2* is an exon of *Wnk1*, we prepared Western blots using whole protein lysates from adult mice, and we separately detected them with an antiserum specific to the C-terminal portion of HSN2 and a purified commercial antibody that recognizes the N terminus of WNK1 (Alpha Diagnostic International) (Figure 2C). Past reports examining WNK1 expression in mouse showed that its MW was slightly greater than 250 kDa (26, 27), and this was confirmed in every tissue detected here with anti-WNK1 (Figure 4, top). By comparison, the anti-HSN2 antiserum detected a band only in tissues of the nervous system, and the MW of this band was smaller (~230 kDa) (Figure 4, middle). The anti-WNK1 antibody failed to reveal any band at approximately 230 kDa in which WNK1/HSN2 was detected with the anti-HSN2 antiserum. To confirm the specificity of the signal detected with the anti-HSN2 antiserum, it was preincubated with its antigenic peptide prior to its use for Western blot and immunohistochemistry detections. This competition step was found to prevent the detection of the approximately 230-kDa band observed in the DRG (Supplemental Figure 1). *WNK1* was previously established to contain 2 distinct promoters (P1 and P2) (25) (Figure 2C), and 2 distinct bands could be observed (~230 and slightly greater than ~250 kDa) when other anti-WNK1 antibodies were used (R&D Systems and Kinasource; Supplemental Figure 2). Together, the detections of Western blots with alternative anti-WNK1 antibodies and the Western blot detection presented in Figure 4 suggest that

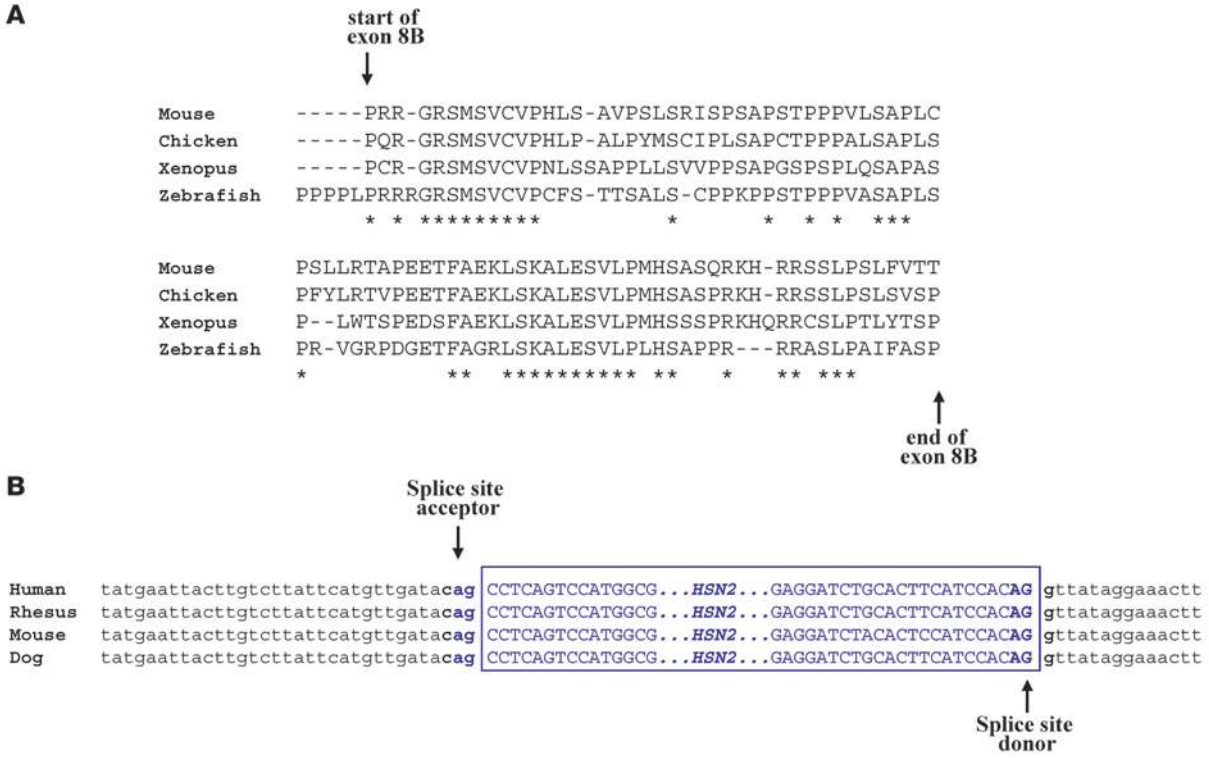

Figure 3
Flanking junction sites of the novel alternatively spliced *WNK1*/*HSN2* isoforms. (**A**) RACE revealed that exon 8B was specifically spliced in some transcripts from mouse brain and spinal cord and the amino acids encoded by this mouse putative exon 8B of the longer *Wnk1*/*Hsn2* isoform are highly conserved across species. A comparison of the amino acids encoded by the exon 8B ORF in the mouse was made with different species/taxa (chicken, *Xenopus*, and zebrafish), and greater than 95% residues are fully or highly conserved (an asterisk below the residues indicates those that are fully conserved across the different taxa/species). (**B**) The amino acid sequences of the splice acceptor and splice donor sites that flank the *HSN2* exon are highly conserved across species. The regions in blue represent the sequence flanking *HSN2*, whereas the regions indicated in black are spliced out during mRNA maturation. Splice acceptor and donor sites are in bold characters. The sequences presented were obtained from the UCSC Genome Bioinformatics Browser (http://genome.ucsc.edu).

it is most likely the second ATG (+640) that is used in the translation of WNK1/HSN2. The 2 alternative polyclonal anti-WNK1 antibodies (Kinasource and R&D Systems) recognize portions of the protein that are downstream to the second ATG, while the anti-WNK1 antibody from Alpha Diagnostic International recognizes a portion (TSKDRPVSQPSLVGSKE) of the protein (14) that is located between the first and the second ATG of the promoters P1 and P2.

Immunohistological investigation of WNK1/HSN2 distribution. While WNK1/HSN2 was observed in both the CNS and PNS, the DRG and sciatic nerves are the tissues with the highest expression (Figure 4). We therefore chose to perform immunohistochemistry to investigate which cells inside the DRG and sciatic nerve expressed WNK1/HSN2. In DRG, the signal was predominantly in the satellite cells that envelop sensory neurons (Figure 5, A and B, arrows), but low expression was also observed in the cell bodies of neurons (Figure 5, A and B, arrowheads). The DRG anti-HSN2 detections were overlaid with parallel detections made using a cocktail of anti–SMI-31 and anti–SMI-32 (neuronal markers). The identity of satellite cells was established with an antibody specific to the glutamine synthetase (28) (data not shown). In cross sections of the sciatic nerve, a strong WNK1/HSN2 signal was visible in the Schwann cells that surround axons (Figure 5D) and in a mosaic distribution of axons (Figure 5, C and D). The same neuron-specific antibodies were used to make parallel detection and overlay images. Given the distribution of WNK1/HSN2-positive axons in the sciatic nerve, which includes fibers from sensory and motor neurons, separate cross sections from both dorsal (Figure 5E) and ventral roots were prepared (Figure 5F). WNK1/HSN2 expression in the 2 roots revealed a striking difference, as the signal was substantially stronger in dorsal roots (almost exclusively containing sensory axons) than in ventral roots (almost exclusively containing motor axons). Given the weak expression of WNK1/HSN2 in the cell body of the DRG neurons, it generally appears that neurons express more WNK1/HSN2 in the axon than the cell body in vivo. To further investigate this, we prepared primary cultures of sensory neurons from DRG and detected these with anti-HSN2 and anti-WNK1 (Alpha Diagnostic International) antibodies. These detections were subsequently overlaid with detections made with the antibodies recognizing the neuronal markers mentioned above (Supplemental Figure 3, A–D). The results showed that in these primary neurons, WNK1/HSN2 is expressed in both the cell body and axons, while WNK1 is only expressed in the cell body and not in the axons. Moreover, immunohistochemistry detection of both DRG and sciatic nerve using anti-WNK1 showed that the protein was ubiquitously expressed in the neuronal somata of the DRG neurons but absent from axonal fibers of sciatic nerve (Supple-

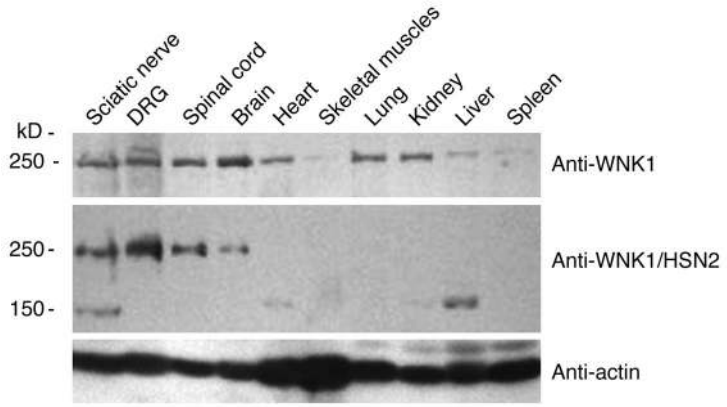

Figure 4
Separate Western immunodetections of WNK1 and WNK1/HSN2. Various mouse tissues from adult or E13 animals were loaded and detected with anti-WNK1 (Alpha Diagnostic International) (top) or with IgG purified anti-HSN2 antibody (middle). Expression of WNK1 was observed in all the lysates, and the expression of WNK1/HSN2 was limited to lysates from neuronal tissues. The membrane detected in the top panel was stripped and then detected with the second antibody. An anti-actin antibody was used to confirm that the loading protein was equal in different lanes (bottom).

mental Figure 3, E–H). The Schwann cells surrounding the fibers of the sciatic nerve express WNK1 (Supplemental Figure 3H, arrow) in addition to WNK1/HSN2 (Figure 5D).

The expression of WNK1/HSN2 in components of the CNS was also investigated by immunohistochemistry (Figure 6). Cross sections of adult mouse spinal cord were prepared and detected with the anti-HSN2 antiserum. In the spinal cord, we observed a strong signal in superficial layers (LI and LII) (Figure 6, A and B), which receive the neuronal projections that carry a variety of sensory information (including most nociceptive information from the PNS). The expression of WNK1/HSN2 also appeared in the fibers of the Lissauer tract (Figure 6B). The neuronal nature of fibers expressing WNK1/HSN2 in LI and LII was confirmed using the neuronal marker SMI (Figure 6B) and a detection using an anti-NeuN antibody (Figure 6D). The axon fibers of dorsolateral funiculus (DLF) and lateral funiculus (LF), which contain ascending sensory fibers, also expressed WNK1/HSN2 (Figure 6, A and B).

Discussion

At the time of the publication of the identification of *HSN2*, the most remarkable feature of this gene was its single-exon structure. The exon mapped within the intron on the same strand and in the same orientation as another gene, *WNK1* (5). While the characterization of the *HSN2* ORF was hampered the existence of an incomplete EST sequence, the ORF was nonetheless found to have three methionines in 5′ and an AATAAA poly(A) addition signal in 3′. While the *HSN2* ORF was novel, *WNK1* had been extensively studied in the context of tissues that are affected in PHAII patients. No symptom overlap was apparent between PHAII and HSANII.

We have now established that *HSN2* is as an alternatively spliced exon of *WNK1* and that this selectively occurs in nervous tissues. The *WNK1/HSN2* nervous system isoforms appear to include either *HSN2* alone or *HSN2* along with a novel exon (putative exon 8B). EST clones encompassing both *Wnk1* and *Hsn2* were previously observed in a mouse E10.5 cDNA library (I.M.A.G.E. 30862659 and 30862741). However, while sequencing these ESTs would have validated our observations, they are no longer available. Prior to this report, only 2 reports examined WNK1 expression in the nervous system (20, 21). In one of them, by Sun et al., neural precursor cells and the anti-WNK1 antibody from Alpha Diagnostic Inter-

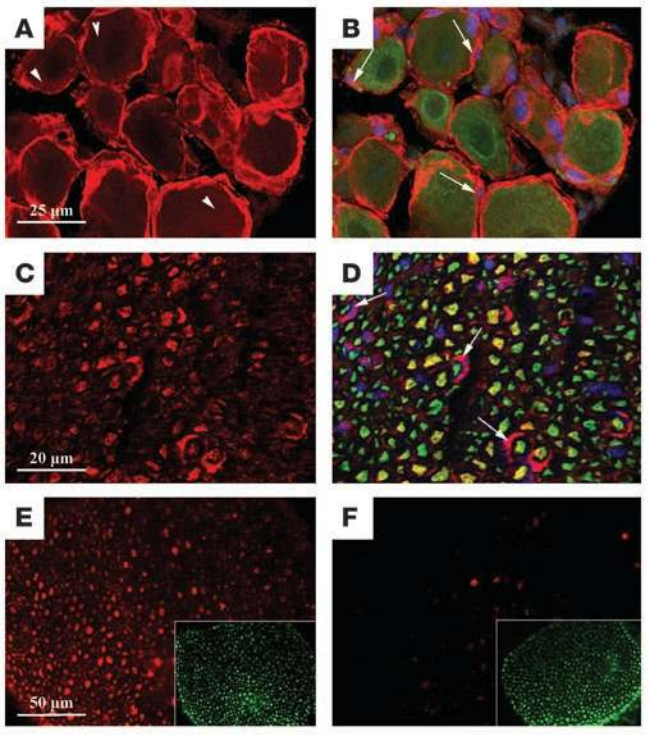

Figure 5
WNK1/HSN2 histological immunodetections. (**A**) Immunohistochemistry detection of adult mouse DRG (from L5 sections) with anti-HSN2 antiserum (red). A clear immunoreactive signal is visible in the satellite cells (arrows) and in some of the neuronal somata (arrowheads). (**B**) Overlaid images of the detections with anti-HSN2 (red in **A**), a mix of axonal markers (SMI-31/32 mix; green), and nuclear staining (TOTO-3 iodide; blue). Colocalization of the signals (yellow overlay) shows that WNK1/HSN2 is expressed in some of the axonal fiber and satellite cells, which surround the neuronal somata (arrows). (**C**) Adult mouse sciatic nerve cross sections detected with the anti-HSN2 antiserum (red) show the presence of the protein in a mosaic distribution of axons. (**D**) Overlaid images of the detection with anti-HSN2 (red in **C**), the axonal markers (green), and nuclear staining (blue) show that not all axonal fibers express WNK1/HSN2 (yellow) and that some do not express WNK1/HSN2 (green). Cross sections of dorsal roots through which sensory axons pass (**E**) and of ventral roots through which motor axons transit (**F**) were detected with anti-HSN2 (red) and the axonal marker (green in **E** and **F**, insets). The majority of motor neuron axonal fibers showed weak or no WNK1/HSN2 signal. In contrast, the HSN2 signal was strong in most of the axonal fibers of the sensory neurons in the dorsal roots. Original magnification of insets, ×400.

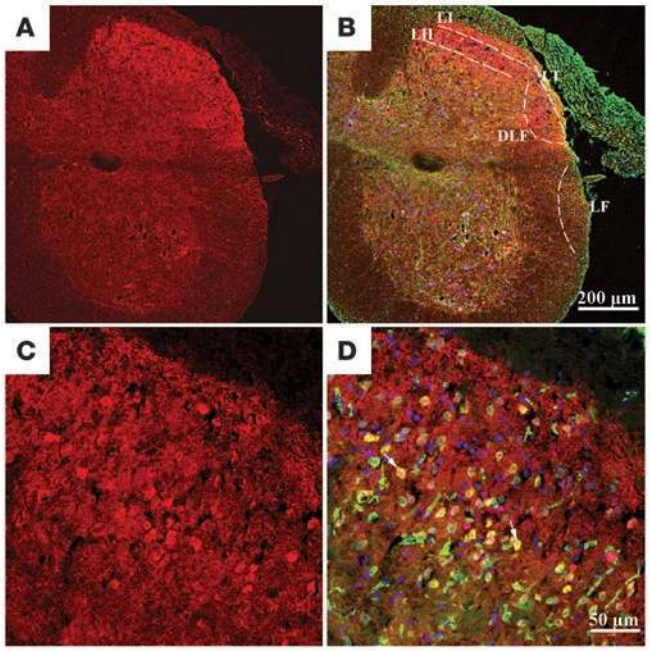

Figure 6
WNK1/HSN2 protein expression in the adult mouse CNS. (**A**) Low-magnification image of immunohistochemistry detections of adult mouse spinal cord cross section with anti-HSN2 antiserum. The anti-HSN2 antiserum gave a strong signal (red) in the superficial layers (LI and LII) of the dorsal horn, the dorsolateral funiculus (DLF), the lateral funiculus (LF), and the Lissauer tract (LT). (**B**) Overlaid images of the HSN2 signal (red in **A**), the signal from the anti–SMI-31/32 axonal marker (green), and the nuclear fluorescent labeling (blue). (**C**) Immunodetection of LI and LII with anti-HSN2 (red). (**D**) Overlaid images of the detection of HSN2 (red in **C**), NeuN (green), and the nuclear labeling (blue). Arrows indicate neurons where the colocalization is observed, confirming the presence of HSN2 protein in cells of this region.

national were used, and a protein said to have a MW of approximately 230 kDa instead of approximately 250 kDa as shown here was observed. It is possible that when Sun et al. identified WNK1, they referred to the antibody specification sheet (catalog WNK11; Alpha Diagnostic International), which indicates that the MW of WNK1 is 230 kDa. However, a number of independent groups reported the MW of WNK1 to be approximately 250 kDa (17, 26, 27, 29). Even though the neuron-specific isoforms (HSN2 alone or HSN2 with exon 8B) of WNK1 incorporate additional amino acids, their MW is nonetheless lower than that of the previously reported WNK1 long isoform, even considering the skipping of exon 11 in the DRG and of exons 11 and 12 in the brain. This lower MW of WNK1/HSN2 is likely attributable to the use of the second promoter (P2) of *WNK1* (25). When the P1 promoter is used, translation is initiated at the ATG (+1), and when the P2 promoter is used, translation is initiated at the more downstream ATG (+640). In both instances the kinase domain of WNK1 is retained, but the use of the second ATG makes the mRNA 642 bp shorter and the protein 214 amino acids smaller. An in vitro study has previously shown that both promoters (P1 and P2) are active and that the second ATG of the P2 promoter is actually sufficiently used to make this form the dominant one in the kidney (25). No examinations have thus far been made in CNS or PNS tissues, but past investigation of the region immediately upstream of the P2 promoter with DNA analysis software (TESS; http://www.cbil.upenn.edu/cgi-bin/tess/tess) identified transcription binding sites that are recognized by neuronal transcription factors (e.g., NF-ATp, HES-1) (21). Unfortunately our 5′RACE reactions did not proceed far enough to provide information about which of the two promoters was used for WNK1/HSN2 transcription. RT-PCR using a primer upstream of the 5′UTR of P1 and a primer in *Hsn2* were prepared with RNA from DRG; the same 5′UTR of P1 primer was used in separate reactions with a primer located in exon 6 of *Wnk1* to amplify kidney cDNA (Figure 2E, arrow 2). The first amplification gave no product (even though long-range PCR conditions had allowed us to amplify larger fragment such as the one between the *Hsn2* and *Wnk1* exon 24). The second amplification, however, produced a fragment of the expected size (~2.5 kb). This suggests that the transcription of *Wnk1/Hsn2* occurs through the second promoter. The comparison of different anti-WNK1 antibodies (Figure 4 and Supplemental Figure 2) also suggested that it is the second ATG that is used to initiate the translation of WNK1/HSN2.

The recessive mutations described in HSANII, here and in previous reports (5–10), all lead to truncations of the WNK1/HSN2 nervous system–specific protein. The disease-causing mutations in *WNK1* identified to date were large, heterozygous intronic deletions that increase the gene expression (11). This impact on the expression level in PHAII patients may explain the absence of hypertension in individuals affected with HSANII, as the expression of the *WNK1* isoform (in which the *HSN2* exon is not incorporated) should not be affected. It is hard to speculate whether some HSANII cases may later be found to have mutations in *WNK1* and not in the *HSN2* portion of *WNK1/HSN2*. However, genetic data presented here suggest that one mutation in the *HSN2* exon is sufficient to cause the HSANII phenotype when combined with a mutation in *WNK1* on the other allele. Moreover, homozygous mutations disrupting *WNK1* isoforms (without *HSN2*) may be lethal, which would explain why all loss-of-function mutations reported to date were located in the *HSN2* exon. A 2003 report supports this possibility, as homozygous mutations of the mouse *WNK1* were shown to be embryonically lethal (30).

While our results indicate that *WNK1/HSN2* is expressed in components of both the CNS and PNS, the HSANII symptoms indicate a defect in peripheral sensory perception. This is consistent with the disease phenotype in which expression of neuronal WNK1/HSN2 appears to be stronger in the sensory neurons than in motor neurons. The primary event of this disorder is liable to occur in sensory fibers, as a very high number of unmyelinated sensory fibers are observed in HSANII. In conjunction with the absence of motor deficit, this constitutes a distinctive pathological hallmark of the disease (31). The expression of WNK1/HSN2 in the outer edge of the DLF, which is where the Lissauer tract travels, may be very relevant for the development of HSANII symptoms, as cells from the Lissauer tract has been reported to be missing in familial, congenital, and universal insensitivity to pain (32, 33). These observations suggest that a more detailed investigation of WNK1/HSN2 expression in components of the posterior horn (e.g., the substantia gelatinosa, where the pain-sensing unmyelinated C fibers are located) (34) at different levels of the spinal cord is needed. Even though no strong evidence supports the hypothesis that myelinating Schwann cells are involved in HSANII, it may eventually be interesting to test whether Schwann cells normally proliferate in

the event of neuronal damage or degeneration. Biopsies of the sural nerve, which contains only sensory fibers, from an HSANII familial case study where multiple affected individuals were diagnosed showed not only a complete absence of myelination but also no evidence of Schwann cell proliferation (35). Based on our observation of WNK1/HSN2 expression in satellite and Schwann cells, it can be hypothesized that the symptoms worsen when these cells respond (28, 36) to the damage sensory neurons suffer because of mutant WNK1/HSN2 expression, although this is speculative. WNK1/HSN2 could act as molecular switch that initiates the proliferation of these cells. In other tissues, WNK1 was shown to activate ERK5 through a MEKK2/3-dependent mechanism, a signaling pathway involved in cell growth and proliferation (18). Though WNK1/HSN2 appears to be expressed predominantly in the PNS, it is also expressed in the CNS. The primary afferents of DRG that transmit sensory stimuli (among them nociceptive) signals are structures that enter the spinal cord through the dorsal root entry zone (DEZ). Once inside the spinal cord, these primary afferents make synapses with second-order neurons of laminae I, II (external; Figure 6A), V, and VI, and from there these fibers take different pathways to transmit HSANII-relevant sensory and nociceptive impulses to structures of the brain stem and diencephalons (37). The gray matter of the spinal cord appeared stained when we used anti-HSN2 and overlaid images of the anti-HSN2 detection and detection of the axonal markers SMI-31/32 (Figure 6), suggesting that any specific HSN2 staining in the gray matter (with the exception of the DEZ) comes mainly from axons, and not cell bodies. The expression of WNK1/HSN2 in the brain was not investigated, but a comprehensive analysis of this will eventually be informative and may help to better understand the disease. Given the strong expression of WNK1/HSN2 in the dorsal roots, it appears probable that the axons of the sciatic nerve expressing this protein are sensory. The difference in the level of WNK1/HSN2 expression observed in the neuronal somata of DRG (Figure 5A) and primary culture prepared from the same DRG (Supplemental Figure 3A) may be the consequence of the activation the neuronal pathway typical of cultured primary neurons. The mechanical, chemical, and new in vitro environment stresses these neurons undergo when the primary culture is established may also activate the expression of WNK1/HSN2. Together, the histological observations suggest that WNK1/HSN2 may have a critical role in the development of the pain-sensory pathways in both the CNS and PNS. WNK1 expression in the PNS during development has not yet been well investigated. Only a few observations made in the CNS were reported, and these showed that WNK1 expression could be seen in the granular layer and cerebellar Purkinje cells, and only weak staining could be observed in the molecular layer and white matter (21). The observation that WNK1 is primarily present in the cell body while WNK1/HSN2 is in the axon may suggest a role in sensory axon maintenance, which is compatible with the neuropathy seen in HSANII.

The sequences of *HSN2* and of the putative exon 8B have no known motif that suggests a particular function, and so how their insertion in *WNK1* affects this protein's function remains to be elucidated. The role of WNK1 in PHAII is partly thought to be attributable to its interaction with WNK4, with ion channels, and with cotransporters through which sodium absorption and potassium wasting is modulated (13). Under normal conditions, WNK1 participates in the regulation of a number of K^+ channels such as ROMK1 (38) and Na^+, K^+, $2Cl^-$, and Na^+Cl^- cotransporters such as NKCCs and NCCs (39). These interactions indicate that WNK1 plays an important role in the regulation of ionic transport across the plasma membrane. In the context of HSANII, it is important to note that the activity of a very relevant ion transporter, TRPV4, is regulated by WNK1 and WNK4 (40). TRPV4 is a vanilloid receptor involved in thermal and mechanical nociception (40). $TRPV4^{-/-}$ mice were found to exhibit hypoalgesic responses to pressures of the tail and acid applications and they have a delayed response to escape from hot temperature (41, 42). How the alternative splicing of *HSN2* and/or of the putative exon 8B to form a nervous system–specific *WNK1/HSN2* isoform affects the normal activity of WNK1 or its affinity for WNK4, TRPV4, or other pain receptors activity is unknown. At this point, it may only be postulated that WNK1/HSN2 is involved in the proper localization and/or ionic regulation of TRPV channels in the nervous system.

Our study of *Wnk1/Hsn2* stresses the importance of tissue-specific alternative splicing, as it shows that mutations in different splice variants may affect protein function differently and consequently lead to very different tissue-specific pathologies. The 9 laminopathies (including lipodystrophies, muscular dystrophies, and progeroid syndromes) that are caused by mutations of the *LMNA/C* gene are good examples of such a phenomenon (43, 44). Unlike the situation with *WNK1*, there is no association between the position or the exon where the mutation occurs and the tissue or system affected.

Methods

Mutation detection. After written informed consent was received from the family, blood samples were collected and DNA was extracted from peripheral blood lymphocytes using a standard protocol. All 28 exons of *WNK1* and the single predicted exon of *HSN2* were amplified by PCR using flanking intronic primers before they were sequenced with an ABI 3700 sequencer, according to the manufacturer's recommended protocol (Applied Biosystems).

RNA isolation and mRNA purification. All animal experiments were approved by the Institutional Committee for Animal Protection (CIPA) of the Centre Hospitalier de l'Université de Montréal. Total RNA was prepared from the different tissues of C57BL/6 adults and E13 embryos according to the method described by Chomczynski and Sacchi (45), and poly(A) RNA was subsequently purified using an Oligotex mRNA Midi Kit (QIAGEN).

Northern blot analyses. Purified poly(A) RNA (2 μg) from the different tissues (C57BL/6 adult and E13 embryo) was electrophoresed on a denaturing formamide/formaldehyde gel and transferred onto a Hybond nylon membrane (GE Healthcare). The membrane was hybridized with a PCR-amplified murine *Hsn2* fragment of 435 bp that recognized the 3′ region of the gene. This 435-bp probe was generated using the primers 5′-CATGCTCAAACACCAAGTTCTT-3′ and 5′-TGAAGCAGATAAGACCTGCTGA-3′ that cover the region found between position 768 and 1,203 bp past the 5′ *Hsn2* spliced-in sequence (Figure 3B). The membrane was also probed with β-actin DNA fragments. Probes were radiolabeled with [α-^{32}P]dCTP–labeled Random prime PCR fragment (Rediprime II Random Prime Labelling System; GE Biosciences). Before use, the fragments were sequenced to confirm their identity. Hybridization was performed according to the procedure previously described by Houle et al. (46). *Wnk1* Northern blotting was performed with an amplified DNA template using 5′-TGACATCGAAATCGGCAGAGGCT-3′ and 5′-GGGTACGGGTAGAATTAGCAGAAG-3′ primers. The probe spans from the end of exon 1 to exon 6 (850 bp).

Analysis of Wnk1 splicing events by RT-PCR. cDNA synthesis and PCR analysis have been described previously by Herblot et al. (47). Total RNA (1 μg) was used as template for first-strand DNA synthesis. Long-range PCR was performed using Long PCR Mix (Fermentas). For each amplification of a specific cDNA, 18S, was coamplified as internal control to correct for variations in loading. Oligonucleotide sequences are listed in Supplemental

Table 1. cDNAs were amplified for 35 cycles, and PCR conditions were: initial denaturation of 94°C for 3 minutes, then 35 cycles of 93°C for 10 seconds, 55°C for 30 seconds, and 68°C for 2 minutes and 45 seconds and then 1 cycle of 68°C for 10 minutes. The amplified fragments were analyzed by agarose gel electrophoresis, and when the sequence of specific bands was investigated, the band was then purified with the QIAEX kit (QIAGEN) and cloned in TOPO PCRII (Invitrogen). Sequence analysis was performed on the ABI 3700 sequencer at the Génome Québec Innovation Centre.

5′RACE assay. RNA was used in conjunction with the GeneRacer kit (Invitrogen) for the 5′RACE and 3′RACE assays. PCR products from the RACE reaction were analyzed on agarose gel and subcloned into TOPO-4 Vector (Invitrogen). Ninety-six clones were chosen, and 23 were sent for sequencing.

Ortholog identification. Orthologous sequences were identified by performing a tBLASTn search of GenBank genome sequences using the peptide sequence encoded by exon 8B of the mouse gene.

Antibody production and immunodetection. DNAstar software version 5.02 was used to examine protein sequence homology, and freely available software (ANTIGENIC; http://immunax.dfci.harvard.edu/Tools/antigenic.html) was used to explore the peptide sequence of HSN2 with good antigenicity. Following these analyses, the best candidate protein sequences were selected for the synthesis of peptides (Sheldon Biotechnology Centre, McGill University) to be used to prepare rabbit polyclonal antibodies at our facilities. An LSPQSVGLHCHLQPVT peptide corresponding to a sequence in the 3′ end of the *HSN2* exon was the one that allowed the preparation of the best antibody in terms of antigenicity and specificity. The peptides were injected with complete and subsequently with incomplete Freund's adjuvant in rabbit to produce an antiserum specific to HSN2 protein (McGill animal facility). Either crude serum (1:1,000) or IgG purified antibody (1:5,000; Montage; Millipore) was used for the Western blot (7.5%) and histological immunodetections. C57BL/6 adult mouse tissues were prepared in SUB lysis buffer (8 M urea, 0.5% SDS, 200 mM β-mercaptoethanol) and resolved by SDS-PAGE. Anti-WNK1 antibody (Alpha Diagnostic International) was used at 1:1,000. The anti-WNK1 made to recognize the kinase domain (Kinasource) was used at 1 μg/ml, and the anti-WNK1 from R&D Systems was used at 0.5 μg/ml. TOTO-3 iodide (Molecular Probes; Invitrogen) was used to generate nuclear staining.

Immunohistochemistry was performed as described previously (48). A cocktail of anti–SMI-31 and anti–SMI-32 (SMI Monoclonals; Covance) was used at 1:1,000 as an axonal marker. Neuronal marker NeuN antibody (Upstate) was used at 1:150. Alexa Fluor 555 secondary anti-rabbit and Alexa Fluor 488 secondary anti-mouse antibodies (Molecular Probes; Invitrogen), respectively, were used (1:1,000) to visualize rabbit and mouse primary antibodies. Our observations were carried out using a Leica TCS SP5 broadband confocal microscope. The system was equipped with the AOBS (acousto-optical beam splitter) for optimal beam splitting. Control immunodetections were made using the preimmunized serum obtained from rabbits, which subsequently yielded the anti-HSN2 antiserum, after their exposure to the HSN2 antigenic peptide, and these did not show a specific signal in either immunohistochemistry or Western blots.

For competition experiments, anti-HSN2 antiserum was incubated with 5-fold excess of its antigenic peptide overnight at 4°C. The same amounts of protein lysates from adult mouse DRG were loaded on a SDS-PAGE and transferred on PVDF membrane. One strip was incubated with anti-HSN2 antiserum alone, and a second strip incubated with the anti-HSN2/peptide mix overnight at 4°C.

Primary cultures of DRG sensory neurons. Adult mouse sensory neuronal cultures were established essentially as described by Seilheimer et al. (49) with some modifications. DRG were dissected from adult mouse C57BL/6 and incubated with 10 mg/ml of collagenase D (Roche) for 45 minutes at 37°C. Trypsin (0.25%) was added at the end of the collagenase D treatment for 30 minutes at 37°C. The tissues were washed once with cold Neurobasal medium (Invitrogen) plus 2% inactivated goat serum and then triturated in warm Neurobasal medium plus serum using fire-polished Pasteur pipettes. One milliliter of the cell suspension was overlaid on 1 ml of 35% Percoll in saline (Pharmacia; Amersham Biosciences) and centrifuged at 10°C at 285 *g* for 15 minutes. The cell pellet, which includes sensory neurons, was washed in 5 ml of fresh medium and resuspended in fresh warm medium with 50 ng/ml of nerve growth factor and plated on pol-D-lysine/laminin–coated coverslips. They were cultured for 48 hours prior to immunocytochemistry. Immunostaining was performed essentially as described previously (50).

Acknowledgments

The authors would like to thank all family members for their cooperation. J.-B. Rivière is the recipient of a Canadian Institutes of Health Research (CIHR) Doctoral Research Award. The CIHR supported G.A. Rouleau with a research grant (IG1-78904) for this project.

Received for publication September 28, 2007, and accepted in revised form April 16, 2008.

Address correspondence to: Guy A. Rouleau, Centre of Excellence in Neuromics, University of Montreal, Centre Hospitalier de l'Université de Montréal, 1560 Sherbrooke East, Room Y-3633, Montreal, Quebec H2L 4M1, Canada. Phone: (514) 890-8000 ext. 24594; Fax: (514) 412-7602; E-mail: guy.rouleau@umontreal.ca.

Masoud Shekarabi and Nathalie Girard contributed equally to this work.

1. Verhoeven, K., et al. 2006. Recent advances in hereditary sensory and autonomic neuropathies. *Curr. Opin. Neurol.* **19**:474–480.
2. Kondo, K., and Horikawa, Y. 1974. Genetic heterogeneity of hereditary sensory neuropathy. *Arch. Neurol.* **30**:336–337.
3. Murray, T.J. 1973. Congenital sensory neuropathy. *Brain.* **96**:387–394.
4. Ota, M., Ellefson, R.D., Lambert, E.H., and Dyck, P.J. 1973. Hereditary sensory neuropathy, type II. Clinical, electrophysiologic, histologic, and biochemical studies of a Quebec kinship. *Arch. Neurol.* **29**:23–37.
5. Lafreniere, R.G., et al. 2004. Identification of a novel gene (HSN2) causing hereditary sensory and autonomic neuropathy type II through the Study of Canadian Genetic Isolates. *Am. J. Hum. Genet.* **74**:1064–1073.
6. Coen, K., et al. 2006. Novel mutations in the HSN2 gene causing hereditary sensory and autonomic neuropathy type II. *Neurology.* **66**:748–751.
7. Takagi, M., et al. 2006. New HSN2 mutation in Japanese patient with hereditary sensory and autonomic neuropathy type 2. *Neurology.* **66**:1251–1252.
8. Cho, H.J., Kim, B.J., Suh, Y.L., An, J.Y., and Ki, C.S. 2006. Novel mutation in the HSN2 gene in a Korean patient with hereditary sensory and autonomic neuropathy type 2. *J. Hum. Genet.* **51**:905–908.
9. Roddier, K., et al. 2005. Two mutations in the HSN2 gene explain the high prevalence of HSAN2 in French Canadians. *Neurology* **64**:1762–1767.
10. Riviere, J.B., et al. 2004. A mutation in the HSN2 gene causes sensory neuropathy type II in a Lebanese family. *Ann. Neurol.* **56**:572–575.
11. Wilson, F.H., et al. 2001. Human hypertension caused by mutations in WNK kinases. *Science.* **293**:1107–1112.
12. Farfel, Z., et al. 1978. Familial hyperpotassemia and hypertension accompanied by normal plasma aldosterone levels: possible hereditary cell membrane defect. *Arch. Intern. Med.* **138**:1828–1832.
13. Xie, J., Craig, L., Cobb, M.H., and Huang, C.L. 2006. Role of with-no-lysine [K] kinases in the pathogenesis of Gordon's syndrome. *Pediatr. Nephrol.* **21**:1231–1236.
14. Xu, B., et al. 2000. WNK1, a novel mammalian serine/threonine protein kinase lacking the catalytic lysine in subdomain II. *J. Biol. Chem.* **275**:16795–16801.
15. Xu, B.E., et al. 2002. Regulation of WNK1 by an autoinhibitory domain and autophosphorylation. *J. Biol. Chem.* **277**:48456–48462.
16. Lee, B.H., et al. 2004. WNK1 phosphorylates synaptotagmin 2 and modulates its membrane binding. *Mol. Cell.* **15**:741–751.
17. Vitari, A.C., et al. 2004. WNK1, the kinase mutated in an inherited high-blood-pressure syndrome, is a novel PKB (protein kinase B)/Akt substrate. *Biochem. J.* **378**:257–268.
18. Xu, B.E., et al. 2004. WNK1 activates ERK5 by an MEKK2/3-dependent mechanism. *J. Biol. Chem.* **279**:7826–7831.

19. Choate, K.A., et al. 2003. WNK1, a kinase mutated in inherited hypertension with hyperkalemia, localizes to diverse Cl- -transporting epithelia. *Proc. Natl. Acad. Sci. U. S. A.* **100**:663–668.
20. Sun, X., Gao, L., Yu, R.K., and Zeng, G. 2006. Down-regulation of WNK1 protein kinase in neural progenitor cells suppresses cell proliferation and migration. *J. Neurochem.* **99**:1114–1121.
21. Delaloy, C., et al. 2006. Cardiovascular expression of the mouse WNK1 gene during development and adulthood revealed by a BAC reporter assay. *Am. J. Pathol.* **169**:105–118.
22. Verissimo, F., and Jordan, P. 2001. WNK kinases, a novel protein kinase subfamily in multi-cellular organisms. *Oncogene.* **20**:5562–5569.
23. O'Reilly, M., Marshall, E., Speirs, H.J., and Brown, R.W. 2003. WNK1, a gene within a novel blood pressure control pathway, tissue-specifically generates radically different isoforms with and without a kinase domain. *J. Am. Soc. Nephrol.* **14**:2447–2456.
24. LeDoux, M.S., et al. 2006. Murine central and peripheral nervous system transcriptomes: comparative gene expression. *Brain Res.* **1107**:24–41.
25. Delaloy, C., et al. 2003. Multiple promoters in the WNK1 gene: one controls expression of a kidney-specific kinase-defective isoform. *Mol. Cell. Biol.* **23**:9208–9221.
26. Wade, J.B., et al. 2006. WNK1 kinase isoform switch regulates renal potassium excretion. *Proc. Natl. Acad. Sci. U. S. A.* **103**:8558–8563.
27. Ohta, A., Yang, S.S., Rai, T., Chiga, M., Sasaki, S., and Uchida, S. 2006. Overexpression of human WNK1 increases paracellular chloride permeability and phosphorylation of claudin-4 in MDCKII cells. *Biochem. Biophys. Res. Commun.* **349**:804–808.
28. Hanani, M. 2005. Satellite glial cells in sensory ganglia: from form to function. *Brain Res. Brain Res. Rev.* **48**:457–476.
29. Zagorska, A., et al. 2007. Regulation of activity and localization of the WNK1 protein kinase by hyperosmotic stress. *J. Cell Biol.* **176**:89–100.
30. Zambrowicz, B.P., et al. 2003. Wnk1 kinase deficiency lowers blood pressure in mice: a gene-trap screen to identify potential targets for therapeutic intervention. *Proc. Natl. Acad. Sci. U. S. A.* **100**:14109–14114.
31. Dyck, P.J. 1993. Neuronal atrophy and degeneration predominantly affecting peripheral sensory and autonomic neuron. In *Peripheral neuropathy*. P.J. Dyck and P.K. Thomas, editors. W.B. Saunders. Philadelphia, Pennsylvania, USA. 1065–1093.
32. Serratrice, G. 1992. Congenital indifference and congenital insensitivity to pain [In French]. *Bull. Acad. Natl. Med.* **176**:609–616; discussion 616–618.
33. Swanson, A.G., Buchan, G.C., and Alvord, E.D., Jr. 1963. Absence of Lissauer's tract and small dorsal root axons in familial, congenital, universal insensitivity to pain. *Trans. Am. Neurol. Assoc.* **88**:99–103.
34. Lu, Y., and Perl, E.R. 2003. A specific inhibitory pathway between substantia gelatinosa neurons receiving direct C-fiber input. *J. Neurosci.* **23**:8752–8758.
35. Basu, S., Paul, D.K., and Basu, S. 2002. Four siblings with type II hereditary sensory and autonomic neuropathy. *Indian Pediatr.* **39**:870–874.
36. Martini, R. 2001. The effect of myelinating Schwann cells on axons. *Muscle Nerve.* **24**:456–466.
37. Almeida, T.F., Roizenblatt, S., and Tufik, S. 2004. Afferent pain pathways: a neuroanatomical review. *Brain Res.* **1000**:40–56.
38. Lazrak, A., Liu, Z., and Huang, C.L. 2006. Antagonistic regulation of ROMK by long and kidney-specific WNK1 isoforms. *Proc. Natl. Acad. Sci. U. S. A.* **103**:1615–1620.
39. Anselmo, A.N., et al. 2006. WNK1 and OSR1 regulate the Na+, K+, 2Cl- cotransporter in HeLa cells. *Proc. Natl. Acad. Sci. U. S. A.* **103**:10883–10888.
40. Dhaka, A., Viswanath, V., and Patapoutian, A. 2006. Trp ion channels and temperature sensation. *Annu. Rev. Neurosci.* **29**:135–161.
41. Suzuki, M., Mizuno, A., Kodaira, K., and Imai, M. 2003. Impaired pressure sensation in mice lacking TRPV4. *J. Biol. Chem.* **278**:22664–22668.
42. Lee, H., Iida, T., Mizuno, A., Suzuki, M., and Caterina, M.J. 2005. Altered thermal selection behavior in mice lacking transient receptor potential vanilloid 4. *J. Neurosci.* **25**:1304–1310.
43. Capell, B.C., and Collins, F.S. 2006. Human laminopathies: nuclei gone genetically awry. *Nat. Rev. Genet.* **7**:940–952.
44. Pollex, R.L., and Hegele, R.A. 2004. Hutchinson-Gilford progeria syndrome. *Clin. Genet.* **66**:375–381.
45. Chomczynski, P., and Sacchi, N. 1987. Single-step method of RNA isolation by acid guanidinium thiocyanate-phenol-chloroform extraction. *Anal. Biochem.* **162**:156–159.
46. Bourgoin, S.G., et al. 2002. ARNO but not cytohesin-1 translocation is phosphatidylinositol 3-kinase-dependent in HL-60 cells. *J. Leukoc. Biol.* **71**:718–728.
47. Herblot, S., Steff, A.M., Hugo, P., Aplan, P.D., and Hoang, T. 2000. SCL and LMO1 alter thymocyte differentiation: inhibition of E2A-HEB function and pre-T alpha chain expression. *Nat. Immunol.* **1**:138–144.
48. Lariviere, R.C., Nguyen, M.D., Ribeiro-da-Silva, A., and Julien, J.P. 2002. Reduced number of unmyelinated sensory axons in peripherin null mice. *J. Neurochem.* **81**:525–532.
49. Seilheimer, B., Persohn, E., and Schachner, M. 1989. Neural cell adhesion molecule expression is regulated by Schwann cell-neuron interactions in culture. *J. Cell Biol.* **108**:1909–1915.
50. Shekarabi, M., et al. 2005. Deleted in colorectal cancer binding netrin-1 mediates cell substrate adhesion and recruits Cdc42, Rac1, Pak1, and N-WASP into an intracellular signaling complex that promotes growth cone expansion. *J. Neurosci.* **25**:3132–3141.